REGENERATIVE BRAKING MONITORING SYSTEM OF ELECTRIC VEHICLE

1st Jusuf Abimas Pratama
Dept. of Electrical Engineering
Sebelas Maret University
Surakarta, Indonesia
15.jusufabimas@gmail.com

2nd Miftahul Anwar
Dept. of Electrical Engineering
Sebelas Maret University
Surakarta, Indonesia
miftahwar@ft.unc.ac.id

3rd Sifaus Wulaning Arsri
Dept. of Electrical Engineering
Sebelas Maret University
Surakarta, Indonesia
sifauswulaninga@gmail.com

4th Ferdiansyah Ashil Farisi
Dept. of Electrical Engineering
Sebelas Maret University
Surakarta, Indonesia
ferdiansyahashil@gmail.com

5th Muhammad Nizam
Dept. of Electrical Engineering
Sebelas Maret University
Surakarta, Indonesia
nizamkh@gmail.com

***Abstract*—Electric vehicles is in rapid development. The energy commonly used as a driving force for electric vehicles comes from batteries. The development of electric vehicle technology is currently concentrated on efforts to charge the battery used by utilizing the power wasted when braking electrically. The gearbox and final drive are installed as a mechanical transmission system for electric vehicles to increase the torque of the BLDC motor as the main driving force of the vehicle. The regenerative process occurs when the Kelly-KBL motor controller electric braking feature is activated. For this reason, Arduino Mega and LabVIEW software are used to observe the current and voltage of lead acid batteries with voltage 48 V and capacity 225 Ah (C20). In addition, a 2 kW BLDC motor RPM was also observed in the electric braking monitoring system. From the results of monitoring and data collection, the vehicle traveled a distance of 36.06 m in 68 s time intervals with an average speed of 16.8 m / s. The average torque value when electric braking on a BLDC motor supplies 154 Nm, while the average torque of the vehicle is 996.99 Nm. The average regenerative power of the wheels is 17.07 kW, while the average mechanical power of the wheels is 13.67 kW. Coulometric state of charge (SOC) shows an increase in battery capacity of 4.27% and 99.97% voltage SOC at the beginning of the activation of the electric brake pedal. Maximum battery power movement when charging, 2.25 kW is caused by the activation of the electric brake pedal. Whereas when using a maximum of 1.52 kW. The application of electric braking has a power consumption efficiency of 0.042%. and charging power charging 18.97%.**

Keywords*— *Electric vehicles, electric braking, regenerative, Arduino Mega, BLDC motor, kontroler Kelly-KBL, LabVIEW, lead acid batteries, power, torque, state of charge (SOC), power efficiency.

I. INTRODUCTION

Electric vehicles are a transportation with alternative fuels that have been popular since the early 20th century. The development of alternative fuel vehicle technology is currently concentrated on efforts to regenerate fuel (electric power) stored in batteries [8, p.299]. Electric vehicles implement an electric braking system that is used to regenerate battery power by utilizing the Back-EMF BLDC motor.

The electric brake pedal will provide an input signal of 0V - 5V to the Kelly-KBL motor controller. The input signal becomes a trigger controller to output the braking current from the battery to the motor. The BLDC motor switches the function into the generator concerned with the Back-EMF braking current generated at each stator winding with a sinusoidal voltage signal [8]. The Back-EMF from the stator will flow through the motor controller to charge the lead acid batteries [7, 11].

Regenerative braking monitoring system is designed using two different devices. LabVIEW software version 2017 functions to calculate, display and store data in the form of documents. LabVIEW is used because it has an interactive display and is easy to program. Arduino Mega hardware functions to retrieve and process data sourced from the output signals of sensors installed in each digital or analog pin. Both devices are integrated with serial communication on the user's personal laptop. The data generated is the basis of the analysis relating to electric braking of electric vehicles to regenerate battery power.

The monitoring system will make it easier for users to find out the vehicle safety. Safeguards in the form of battery disconnection and replacement of fuse components with higher values can be performed by the user if the current and voltage displayed are higher than the specified limits in the motor and battery controller specifications. The analysis of efficiency using electric brakes to regenerate battery power is calculated from input on rear wheel devided by output on battery.

II. METHOD

A. Electric Vehicle

Electric vehicles use batteries as the main power source so the distance depends on the capacity of the battery. The lowest distance that can be traveled by electric vehicles according to the New European Driving Cycle (NEDC) is 85-528 km, while the power consumption is between 117-268 Wh/km [3, p.1]. The distance is influenced by conditions, driving style, road conditions, climate, vehicle system configuration, battery type and usage life [4].

On the other hand, electric vehicles have their own advantages in terms of simplicity of construction, operation and comfort. This type of vehicle is also free emissions with a relatively low noise level, making it environmentally friendly. Electric propulsion provides instant high electromagnetic torque, even at low speeds [4, p.4]. These advantages and limitations make electric vehicles only suitable for use in residential areas or amusement parks.

Electric vehicles have a combination of devices that support vehicle operation [4, p.2]. These devices can be classified into two systems, namely electrical systems and mechanical transmission systems. The systems are integrated, which could be seen in Fig. 1.

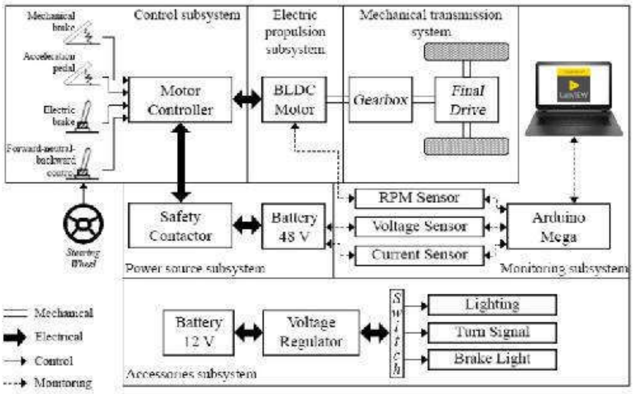

Fig. 1. Electric vehicle system configuration [2, p.100]

Electrical system consists of various components which are divided into several subsystems, which are presented in Table 1.

TABLE I. COMPONENTS IN ELECTRICAL SYSTEMS

Electrical System	Electrical Components
Power source subsystem	6 V 225 Ah 20 h lead acid battery (8 battery in series configuration)
	Safety contactor
Control subsystem	Kelly-KBL motor controller
	Acceleration pedal
	Mechanical brake
	Electric brake
	Forward-neutral-backward control
Electric propulsion subsystem	2 kW outrunner BLDC with hall effect sensor
Monitoring subsystem	Arduino Mega
	Voltage sensor
	Current sensor
	RPM sensor
Accessories subsystem	Lighting
	12V battery
	Turn signal
	Brake light
	Steering Wheel
	5V voltage regulator

Transmission using a chain and prime mover inrunner BLDC motor in electric vehicles was implemented by Kukuh Baharudin in 2018 [7]. At present the transmission system is replaced with the gearbox transmission system and the BLDC outrunner motor as the prime mover. This electric vehicle applies a rear wheel drive system, so the gearbox is placed behind the vehicle, just above the axle. The mechanical transmission system of electric vehicles is presented in Table 2.

TABLE II. COMPONENTS IN MECHANICAL TRANSMISSION SYSTEMS

Mechanical Transmission System	Transmission Type	Gear Rasio (A : B)	Coefficient Rasio (k)
Gearbox	Chain	2,25:1	2,25
	Single speed gear	1:2	0,5
	Chain	1:2,14	0,48
Final Drive	Differential gear	-	2,35
	Rear wheel	-	-

In Fig. 2, electric vehicles have been developed by the Mechanical Engineering Diploma since 2017, followed by a group of students from the Electrical Engineering which is focused on the electrical parts of vehicles including batteries and electric motors.

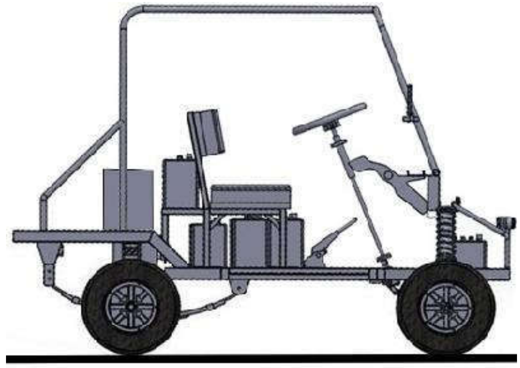

Fig. 2. Electric vehicle

The weight and size of the electric vehicles are in Table 3 as follows.

TABLE III. WEIGHT AND SIZE

Vehicle Weight		Vehicle Size	
Description	***Unit***	***Description***	***Unit***
Battery pack	± 158.4 kg	Height	1,68 m
Chassis	± 300 kg	Width	1,33 m
Gearbox	± 35 kg	Wheel diameter	0,48 m
Wheel	± 166,6 kg		
Two passenger	± 140 kg		
Sum Total	± 800 kg		

B. *Monitoring System*

Monitoring is broadly defined as the cycle of collecting, reviewing, analyzing, evaluating and acting based on stored data. Regenerative braking monitoring system on LabVIEW and Arduino Mega was developed as an additional system to monitor the voltage, current, and RPM from battery to BLDC motors. In Fig. 1 monitoring subsystem, LabVIEW is used as software and Arduino Mega is used as hardware.

The software LabVIEW is an user interface that could display in the form of graphs and save all data from hardware. Data saving features will make it easier for users to do mechanical and regenerative power analysis of electric vehicles. There is an interface menu to display a warning message that is useful for taking safety precautions in the event of an excess battery voltage. The interface menu could be seen in Fig. 3.

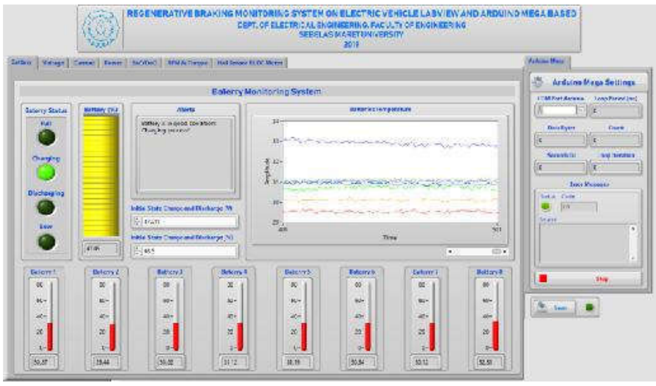

Fig. 3. Monitoring system on LabVIEW interface

The hardware Arduino Mega is an microcontroller that connected to sensors for reading voltage and current battery value, also the RPM speed of BLDC motor. Sensors are needed for monitoring and analysis activities, which is a device that is needed to receive and respond to signals [6, p.1]. The schematic of Arduino Mega with sensors could be seen in Fig. 4.

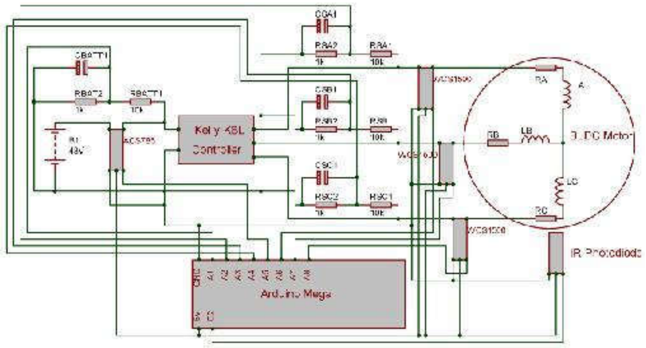

Fig. 4. Subsystem monitoring schematic Arduino Mega with sensors

The voltage sensor uses a voltage divider resistor and a capacitor. The voltage divider resistor functions to reduce the voltage of the lead acid battery so that it can be measured by Arduino Mega. For DC voltages with relatively low frequencies, the voltage divider circuit is quite accurate, where the frequency response over a wide range is fast enough. Voltage divider resistors need capacitive elements to compensate for load capacitance, the device used is a capacitor.

ACS758 is a device for measuring AC or DC currents by contact, while WCS1500 is not contact. Both devices are commonly used for close loop control, where ACS758 and WCS1500 will provide feedback signals in the form of steady state errors. In the regenerative braking monitoring system of electric vehicles, the two sensor devices are used to measure the amount of current in the lead acid batteries and the three-phase BLDC motor controller.

The device for identifying infrared light is called the photodiode infrared (IR-Photodiode) sensor which is available in the form of modules. The sensor is placed next to the BLDC motor with a distance of about 3 cm.

C. Mathematical Equations

Equations are statements that express the equations of two mathematical expressions. Equations have the equal sign, right-side expressions and left-side expressions. Mathematical equations are used to analyze data stored by the monitoring system.

The first equation is to get revolutions per minute (RPM) value. RPM describes the movement of a BLDC motor that moves at a constant speed in a circle of radius r in the Tppr period as the time interval required for one full rotation of a BLDC motor as shown in Fig. 5 [10, p.92]. The mathematical equation used for the calculation of RPM is expressed as the following [9].

$$n_{mtr} = (PPR \times 60000)/T_{PPR} \quad (1)$$

PPR is calculated if the IR-Photodiode sensor is passed by the white part of the rotating motor shaft, T_{ppr} is the time function millis (ms) of Arduino Mega minus oldtime as the final time of PPR calculation. The value of 60000 is the conversion of millisecond units to minutes.

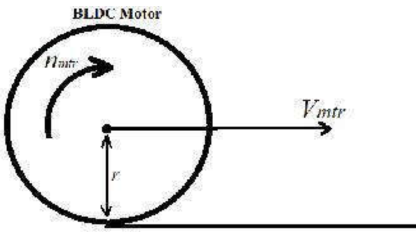

Fig. 5. BLDC motor RPM

Based on Fig. 5, the conversion of RPM to linear velocity (m/s) the following equation is used [2, p.1].

$$v_{mtr} = n_{mtr} \times (2 \times \pi \times r)/60 \quad (2)$$

Fig. 6. Torque and speed flow diagram in gearbox

In Fig. 6, speed and torque will change when accelerating. Gearbox in Table 2 has a coefficient of gear rasio, where in chain 1 there is an r_1 as gear A with input speed originating from motor speed v_{mtr}. Gear A connected to pinion r_2 as gear B using a chain producing output speed v_{out1} by the following equation.

$$v_{out1} = k_1 \times v_{mtr} \quad (3)$$

On the single speed gear section there is a Z_1 as gear A with input torque and input speed originating from the v_{out1}. Z_1 rotation is in the opposite direction with Z_2 as pinion gear B, produces a output speed v_{out2} by the following equation.

$$v_{out2} = k_2 \times v_{out1} \quad (4)$$

On the chain 2, in which there are r_1 as gear A and r_2 as gear B. r_1 has input speed coming from a single speed gear output speed v_{out2}. r_2 is a pinion gear with output speed v_g as final output speed of gearbox to axle and wheels (final drive). The equation for v_g as follows.

$$v_g = k_3 \times v_{out2} \quad (5)$$

In Table 2, the chain 2 chain in the gearbox provides speed v_g to differential gear as v_d with a differential ratio (k_d). The differential gear speed v_d is obtained by the following equation.

$$v_d = k_d \times v_g \quad (6)$$

If the electric vehicle going straight, the differential gear speed v_d will be halved evenly towards the right wheel and left wheel with the following equation.

$$v_w = v_{wl} = v_{wr} = v_d/2 \quad (7)$$

Force F causes acceleration of the mechanical component on vehicle. Based on Newton's second law, the force on a vehicle can be calculated by multiplying the weight of the vehicle m (in Table 3) by acceleration a with the following equation [1, p.142].

$$F = m \times a \quad (8)$$

Then, to calculate the average acceleration can be done with the following equation [1, p.18].

$$a = dv/dt \quad (9)$$

The rotating force of a BLDC motor creates mechanical torque affected by the radius of the BLDC motor or wheel r in the following equation [12, p.7].

$$T = r \times F \quad (10)$$

Mechanical torque produced by the BLDC motor will be affected by the gearbox and final drive, so r is equal to gear rasio coefficient k. Thus, the equation as follows.

$$T = k \times F \quad (11)$$

To calculate the ratio of displacement or distance used the following equation in the form of infinite integrals (or antiderivatives) in both segments in the equation as follows [1, p.25].

$$\int ds_w = \int v_w \ dt \quad (12)$$

The next equation is converting hall effect signals from the ACS758 and WCS1500 sensors to current value. The mathematical equation to calculate the amount of current is as follows [5].

$$Vpp = ((maxValue - minValue) \times 5)/1024 \quad (13)$$

Then,

$$I_{batt} = ((Vpp/2) \times 1000)/sensitivity \times I_{calib} \quad (14)$$

The voltage value based on the voltage divider sensor is calculated using the following mathematical equation.

$$V_{batt} = V_{sensVal} \times (5/1024) \times V_{calib} \quad (15)$$

After get the amount of current and voltage by sensors, the important parameter for lead acid batteries analysis is State-of-Charge (SOC). SOC could be defined as the ratio of remaining capacity to fully charged capacity in hour unit. Changes to SOC are stated with equation as follows [8, p.302].

$$\Delta SOC = I_{batt}/Q(i_{C20}) \ dt \quad (16)$$

Charging or discharging occurs during the time interval in certain voltage besides current. This means that a fully charged battery has 100% SOC and an empty battery has 0% SOC [8, p.302]. When discharging the positive battery current and when charging a negative battery current. Thus, the battery SOC can be calculated with the initial value of V_{min} and final value V_{max} in the following equation.

$$SOC = 100 \times (V_{batt} - V_{min})/(V_{max} - V_{min}) \quad (17)$$

For electric vehicles, power capacity is considered more important than coulometric capacity (Ah) [8, p.302], because it is directly related to dynamic vehicle operation. V_{batt} is a voltage symbol and I_{batt} is a current symbol at the battery terminal. Battery power can be expressed with the following mathematical equation [2, p.302].

$$P_{batt} = V_{batt} \times i_{batt} \quad (18)$$

Mechanical power is different from battery power, affected by mechanical components on electric vehicles. Power in a mechanical component of a vehicle with the following equation [1, p.156].

$$P = F \times v \quad (19)$$

With the calculation of battery power and mechanical power, regenerative braking can be observed by the change in mechanical power from the wheel rotation as input to electric power on battery power as output for reuse to accelerate. In which could be shown in Fig. 7.

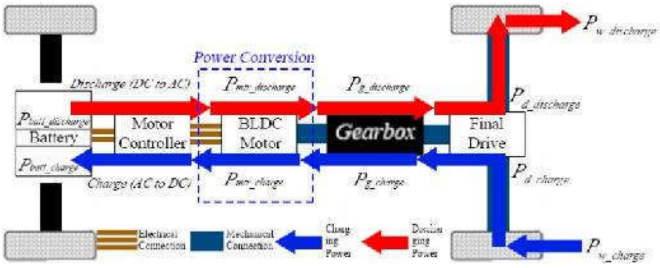

Fig. 7. Power flow diagram on electric vehicles

Power losses during discharging and charging the battery appear in the form of mechanical losses. Therefore, battery efficiency during discharging and charging can be calculated at a certain point of electric braking (deceleration) as the ratio of wheel power as input to battery power as output. Battery efficiency when discharging is calculated by the following equation.

$$\eta_{discharging} = P_{w\ disharge}/P_{batt\ disharge} \quad (20)$$

and battery efficiency when charging is calculated by the following equation.

$$\eta_{charging} = P_{batt\ charge}/P_{w\ charge} \quad (21)$$

The battery is estimated to have high discharging efficiency with high SOC and high charging efficiency with low SOC. Therefore, the Kelly-KBL controller unit must control the battery SOC in its middle range to improve operating efficiency and reduce the temperature rise caused by power losses.

III. Data Analysis

The data generated by the monitoring system are battery voltage, battery current and motor RPM. One way to analyze data is to look for a constant value or average value. Calculated by dividing the accumulated data by the amount of data (number of data samples). This chapter is an analysis of data based on the following mathematical equation.

A. Analysis of Gearbox and Final Drive Effects

The installation of the gearbox and final drive causes changes in speed and torque. Changes that occur is decrease or increase in the value of the speed and torque flowing from the BLDC motor to the wheels as in Fig. 6 about the flow of speed and torque of vehicles. The speed value is obtained from (2), then recalculated with the coefficients listed in Table 2. The change in speed can be seen in figure as follows.

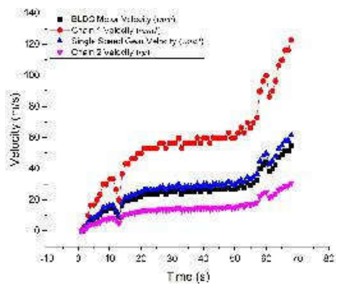

Fig. 8. Speed change on the gearbox

From Fig. 8, the BLDC motor speed is smaller than chain 1 ($v_{mtr} \leq v_{out1}$). Chain speed 1 is greater than single speed gear ($v_{out1} \geq v_{out2}$). Single speed gear speed is greater than chain 2 ($v_{out2} \geq v_g$).

Final drive consists of differential gear and wheels as shown in Fig. 1. The speeds of the two mechanical components are obtained from (6) and (7). The speed of the final drive is shown in figure as follows.

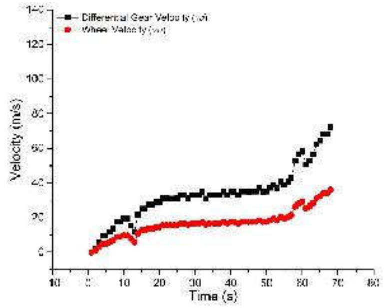

Fig. 9. Change in speed on the final drive

The differential gear speeds are distributed to the right wheel and the left wheel, so the speeds on both wheels are the same, referred to as v_w. From Fig. 9, the differential gear speed is greater than the wheel speed ($V_d \geq V_w$).

Based on the data shown in Fig. 8 and 9, the average v_{mtr} is 25.41 m/s, while the average v_w is 16.8 m/s. Thus, the installation of the gearbox as a mechanical transmission system for electric vehicles causes a decrease in the speed of the BLDC motor.

The torque is obtained from (10) and (11), the radius of the BLDC motor and the wheel of the vehicle are the same. But the gear radius is assumed to be equal to the gear ratio coefficient in the gearbox and final drive. The results of the torque calculation are shown in figure as follows.

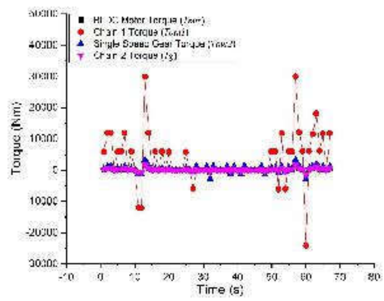

Fig. 10. Torque change on the gearbox

Fig. 10 shows that the torque of a BLDC motor is smaller than chain 1 ($\pm T_{mtr} \leq \pm T_{out1}$). Chain 1 torque is greater than single speed gear ($\pm T_{out1} \geq \pm T_{out2}$). Single speed gear torque is greater than chain 2 ($\pm T_{out2} \geq \pm T_g$).

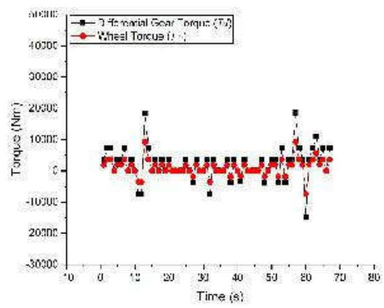

Fig. 11. Torque change on the final drive

Fig. 11 also shows the same torque movement characteristics as Fig. 10. The differential gear torque is evenly distributed to the right wheel and left wheel. Therefore, the differential gear torque to give rotation to the wheels has greater value ($\pm T_d \leq \pm T_w$).

The resulting torque graph is very dynamic due to the operation of the electric brakes. It can be seen that the torque is positive and negative. When the electric brake is active, negative torque will slow down the speed of the wheel. The analysis of torque rotational direction is relative because gear rotation varies for forward and reverse vehicle conditions, in the other hand regenerative brake is happened in discrete time.

Based on the data shown in Fig. 10 and 11, the average BLDC T_{mtr} is 154 Nm, while the average T_w vehicle is 996.99 Nm. Thus, the installation of the gearbox as a mechanical transmission system for electric vehicles causes an increase in BLDC motor torque.

B. Vehicle Speed and Acceleration Analysis

BLDC motor RPM data generated by the regenerative braking monitoring system is useful in calculating the distance, speed and mechanical acceleration of electric vehicles. To calculate the vehicle's mileage, the speed data is reprocessed to get the value of the wheel speed after going through the gearbox and final drive. Distance achieved during data collection is calculated based on (12).

When the acceleration changes with a positive value, the vehicle is said to experience acceleration [1, p.19]. If the vehicle acceleration changes with a negative value, then the vehicle is said to experience deceleration. The results of calculating the distance, speed and acceleration or decceleration of the vehicle are shown in figure as follows.

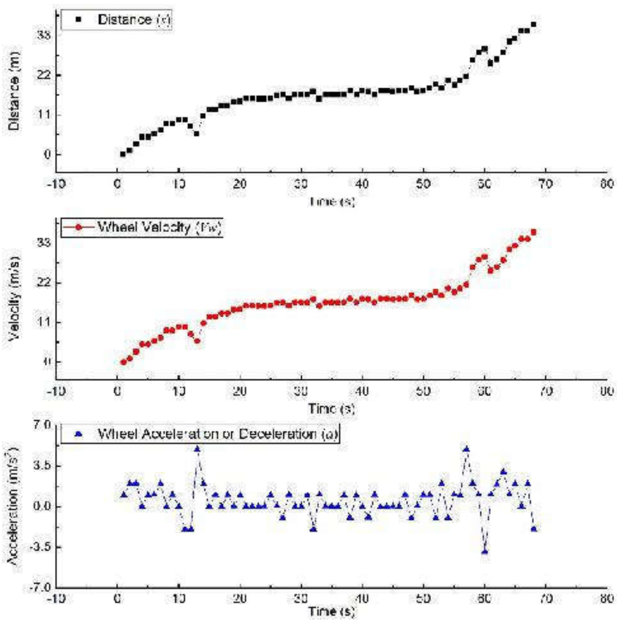

Fig. 12. Distance, speed and acceleration of electric vehicles

From Fig. 12, the speed and distance have the same value. Electric vehicles travel a distance of 36.06 m in 68 s time intervals. Electric vehicles drove with an average speed of 16.86 m/s during data collection. The average acceleration at a certain time t is 1.04 m/s^2. The average deceleration at a particular time t is 1.73 m/s^2.

Electric vehicle slowdown is affected by negative value torque when the electric braking takes place. In other words, the current flowed by the controller is opposite to the wheel torque. Thus, the electric brake to slow down the speed of the vehicle is functioning.

C. Vehicle Force and Power Analysis

Force is an important factor in the analysis of vehicle torque and power. The force is calculated by (8), influenced by the weight of the vehicle in Table 3 and the acceleration or deceleration in each gearbox and final drive component. Torque analysis in Fig. 10 and 11 has been done with the force affected by the BLDC motor radius and gear ratio coefficient. The results of the force calculation on the gearbox are shown in figure as follows.

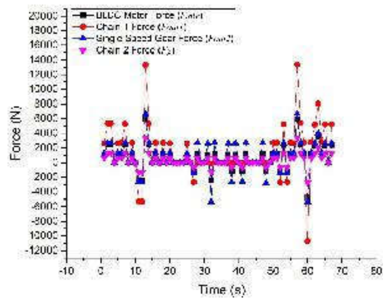

Fig. 13. Force change on the gearbox

In Fig. 13, the BLDC motor force is smaller than chain 1 ($\pm F_{mtr} \leq \pm F_{out1}$). Chain force 1 is greater than single speed gear ($\pm F_{out1} \geq \pm F_{out2}$). Single speed gear force is greater than chain 2 ($\pm F_{out2} \geq \pm F_g$).

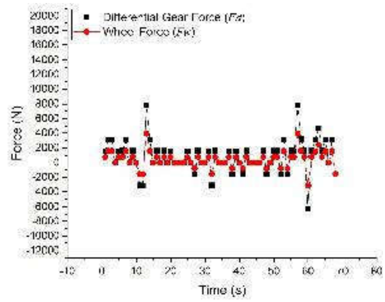

Fig. 14. Force change on the final drive

Fig. 14 shows the force affected by vehicle acceleration. The differential gear force is larger than the wheel force ($\pm T_d \geq \pm T_w$). The average force of a BLDC motor is 641.89 N, while the average force of a vehicle's wheels is 401.65 N. The decrease in force is influenced by the acceleration of each gearbox and final drive component.

Mechanical power is calculated by (19), based on the force and speed of each gearbox and final drive component. The results of the force calculation are shown in figure as follows.

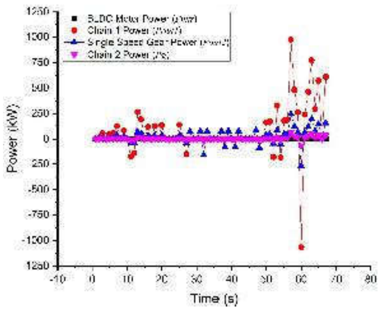

Fig. 15. Power change on the gearbox

In Fig. 15, BLDC motor power is smaller than chain 1 ($\pm P_{mtr} \leq \pm P_{out1}$). Chain power 1 is greater than single speed gear ($\pm P_{out1} \geq \pm P_{out2}$). Single speed gear power is greater than chain 2 ($\pm P_{out2} \geq \pm P_{g}$).

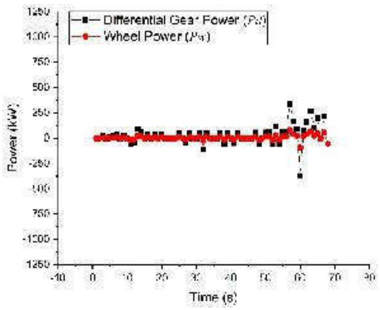

Fig. 16. Power changes on the final drive

Fig. 16 shows the amount of power that is affected by vehicle acceleration. The differential gear power is greater than the wheel power ($\pm P_{d} \leq \pm P_{w}$). The average power of a BLDC motor is 15.57 kW, while the average power of a vehicle's wheels is 5.98 kW. The increase in power value is influenced by the speed of each gearbox and final drive component.

Mechanical power in a wheel can be used as a predictive value of the power generated for regenerative batteries. The mechanical negative power of a wheel is an indicator of a regerative power for charging and the positive power is for discharging batteries. The mechanical power data is separated into figure as follows.

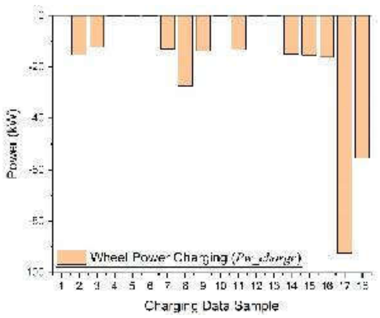

Fig. 17. Regenerative power of a wheel for charging batteries

The regenerative power during electric braking comes from wheel to the batteries for charging. In Fig. 1, it can be seen that the wheel is mechanically connected from the differential gear to BLDC motor, while the connection between BLDC motor to batteries is electrically. The 17th sample data increasing significantly from the regenerative power trend. The value of the 17th sample data is -92.31 kW. Therefore, it is necessary to calculate the average value of the regenerative power of a wheel because of the fluctuated data. So that the average regenerative power from wheel is obtained 17.07 kW.

The mechanical power during electric braking comes from batteries to the wheel, named discharging. In Fig. 18, the 41st sample data shows different values from the regenerative power trend. The value of the 41st sample data is 84.23 kW. The average mechanical power on the wheel is obtained 13.67 kW.

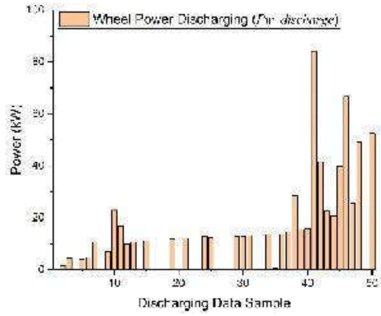

Fig. 18. Mechanical power of a wheel for discharging batteries

D. Battery Power and State of Charge (SOC) Analysis

State of Charge (SOC) increased capacity of lead acid batteries (C20 = 225 Ah) during electric braking [8, p.302]. With a capacity Q at constant current i_{C20} instead of 11.25 A, changes in the value of SOC are calculated based on the equation 16 results as follows.

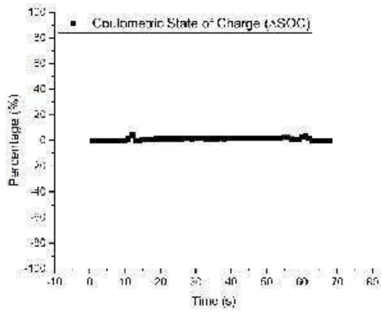

Fig. 19. State of Charge (SOC) of lead acid batteries based on current

Fig. 19 shows the movement of SOC in coulometric, meaning that battery capacity increasing 4.27% at the beginning of the activation electric brake pedal. SOC moves dynamically until touched the value of 0% due to the movement of current entering or exiting the battery to the controller during electric braking. The Kelly-KBL controller releases the braking current which slows the wheel acceleration rate.

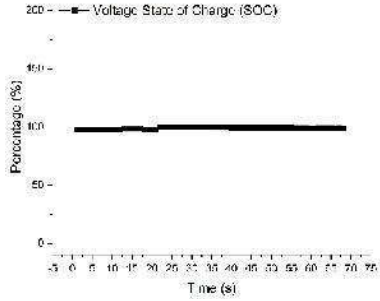

Fig. 20. State of Charge (SOC) of lead acid batteries based on voltage

From Fig. 20, the maximum SOC value of 99.97% is caused by an increasing battery voltage when the electric brake pedal is activated for the first time. SOC affects the battery charging power during electric braking. SOC moves down because the battery power is consumed by the BLDC motor to deccelerates wheel acceleration.

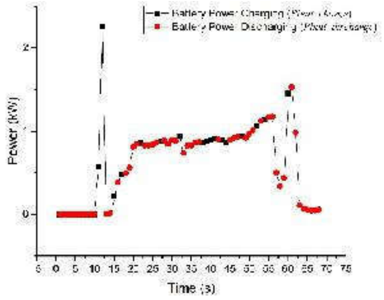

Fig. 21. Lead acid batteries power change

Fig. 21 shows the movement of battery power with a maximum charging value of 2.25 kW caused by the activation of the electric brake pedal. Dynamic moving power follows the charging and discharging current and voltage from the battery to the controller to release braking power which slows the vehicle's speed. The maximum value of discharging is 1.52 kW. The electric power in a battery can be classified according to the mechanical negative power of the wheel is an indicator of the regenerative power for charging and positive power for battery discharging. Battery power data is separated into pictures as follows.

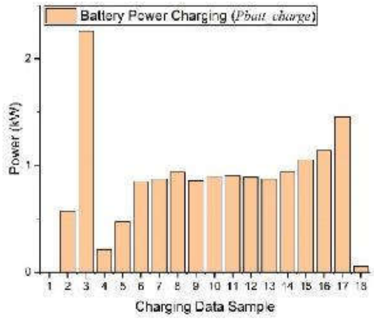

Fig. 22. Lead acid batteries power during charging

Fig. 22 shows the charging data sample of battery power with a maximum charging value is 2.25 kW in the 3rd sample data caused by the activation of the electric brake pedal. The average charging power to batteries is obtained 0.9 kW.

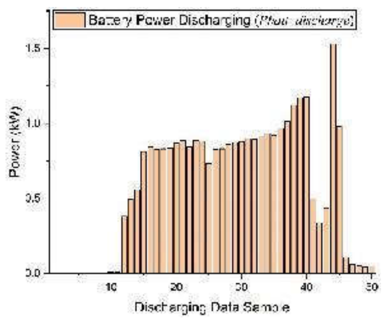

Fig. 23. Lead acid batteries power during discharging

Fig. 23 shows the discharging data sample of battery power with a maximum discharging value is 1.52 kW in the 44th. The average power discharging from batteries is obtained 0.57 kW.

The efficiency of electric braking can be mathematically analyzed by the ratio of wheel mechanical power to battery power (20) when charging and battery power to wheel mechanical power by (21) when discharging. Power of battery and wheel for calculated the efficiency is constant. So the power efficiency when charging is 18.97% and discharging is 0.042%.

IV. Conclusion

The electric brake system have low charging efficiency and very low discharging efficiency with high State of Charge (SOC). Vehicles travel a distance of 36.06 m in 68 s time intervals. Mechanical power value increased by the speed of each gearbox and final drive component. The average regenerative power from a vehicle's wheel is 17.07 kW and average mechanical power to the wheel is obtained 13.67 kW. In the others, the average charging power of batteries is 0.9 kW and the average power discharging from batteries is obtained 0.57 kW. The maximum SOC value is 99.97%, caused by an increasing battery voltage when the electric brake pedal is activated for the first time. Whereas the power efficiency when charging is 18.97% and discharging is 0.042%. Therefore, the controller unit could be re-program to control the battery power during electrical brake in its middle range to improve operating efficiency and reduce the temperature rise caused by power losses.

Acknowledgment

This work was partially supported by Grants-in-Aid from Kemenristekdikti for scientific research (PUSNAS 1729a/UN27.21/PP/2017) and PNBP UNS (Fundamental Research 516/UN27.21/PP/2019).

References

[1] D. Halliday, R. Resnick, and J. Walker, Fundamentals of Physics, 9th Editio. United States of America: John Wiley & Sons, Inc., 2011.

[2] D. K. Neal, "Angular Velocity vs. Linear Velocity," Bowling Green, KY, 117.

[3] E. A. Grunditz and T. Thiringer, "Performance Analysis of Current BEVs Based On A Comprehensive Review of Specifications," IEEE Trans. Transp. Electrif., vol. 2, no. 3, pp. 270–289, 2016.

[4] F. Un-Noor, S. Padmanaban, L. Mihet-Popa, M. N. Mollah, and E. Hossain, "A comprehensive study of key electric vehicle (EV) components, technologies, challenges, impacts, and future direction of development," Energies, vol. 10, no. 8, pp. 1–82, 2017.

[5] Henry, "ACS758 Arduino Current Sensor Tutorial," Henry's Bench, 2015. [Online]. Available: http://henrysbench.capnfatz.com/henrys-bench/arduino-current-measurements/acs758-arduino-current-sensor-tutorial/. [Accessed: 17-May-2019].

[6] J. Fraden, Handbook of Modern Sensors, Fifth Ed. San Diego, CA, USA: Springer, 2015.

[7] K. Bahrudin, "Sistem Transmisi Pada Mobil Golf Listrik," Universitas Sebelas Maret, 2018.

[8] M. Ehsani, Y. Gao, S. E. Gay, and A. Emadi, Modern Electric, Hybrid Electric, and Fuel Cell Vehicles. CRC PRESS, 1385.

[9] Opto, "RPM Measurement Techniques," Temecula, CA, Form 1784-160609, 2016.

[10] R. A. Serway and J. W. J. Jr., Physics for Scientists and Engineers with Modern Physics, 9th ed. Boston, MA: Brooks/Cole Cengage Learning, 2014.

[11] Y. Gao, L. Chen, and M. Ehsani, "Investigation of the Effectiveness of Regenerative Braking for EV and HEV." SAE International, 1999.

[12] Y. Liklikwatil, Mesin-mesin Listrik, Ed.1. Yogyakarta: Deepublish, 2014.